THE JOURNAL OF PHYSICAL CHEMISTRY LETTERS
A JOURNAL OF THE AMERICAN CHEMICAL SOCIETY

pubs.acs.org/JPCL

Letter

Observation of an Excited Dipole-Bound State in a Diatomic Anion

Yuzhu Lu, Rulin Tang, and Chuangang Ning*

Cite This: *J. Phys. Chem. Lett.* 2021, 12, 5897−5902

Read Online

ACCESS | Metrics & More | Article Recommendations

ABSTRACT: We report the observation of σ-type and π-type excited dipole-bound states (DBSs) in cryogenically cooled potassium iodide (KI) anions for the first time. Two DBSs were observed 39.7(10) meV and 5.0(12) meV below the photodetachment threshold via the resonant two-photon detachment. The different photoelectron angular distributions and binding energies suggest that the two DBSs are of different types. The existence of one σ-type and one π-type DBS in the KI anion was also supported by the high-level *ab initio* theoretical calculations. The excellent agreement between experimental and theoretical results confirms the prediction that a dipolar molecule with a large enough dipole moment can have an excited DBS.

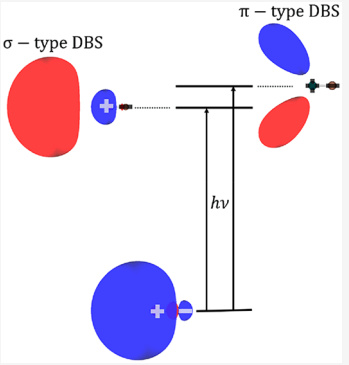

Downloaded via TSINGHUA UNIV on June 22, 2021 at 07:01:22 (UTC).
See https://pubs.acs.org/sharingguidelines for options on how to legitimately share published articles.

A polar molecule with a sufficiently large dipole moment can bound an extra electron to form a dipole-bound anion. The extra electron resides in a very diffuse orbital with low binding energy due to the shallow long-range electric dipole potential well.[1−5] The dipole-bound state (DBS) can serve as the "doorway" of some electron attachment processes,[6−10] and is important for varieties of biological molecules[11−15] and interstellar molecules.[16,17] Theoretical investigations on the binding of an electron to an electric dipole dates back to 1947, when Fermi and Teller first gave the critical dipole moment of 1.625 D.[18,19] More refined calculations and experiments show that the empirical critical dipole moment for molecules to support a DBS is about 2.5 D.[1,3,5,20−23] A real dipolar molecule usually has only one DBS due to the shallow potential well. However, theories predicted that a molecule with a large enough dipole moment could have more than one DBS.[3,24−27] The critical value for having an excited π-type DBS is 9.6 D, according to the results of the finite dipole model.[3,28,29] Up to now, almost in all experiments of polar molecules, only one DBS for each molecule has been observed, and it is σ-type, except the recent work by Yuan et al.[30,31] They reported the existence of a π-type DBS indicated by photoelectron angular distributions of deprotonated 9-anthrol (9AT, $C_{14}H_9O$) molecular anions. The dipole moment of 9AT is 3.6 D, and only one DBS was observed. The π-type DBS was believed to be stabilized by the large anisotropic in-plane polarizability of 9AT.[30]

To observe excited DBSs, we focused on the highly polar alkali−halide diatomic molecules MX (M = Li, Na, K, Rb, Cs; X = F, Cl, Br, I). The simple electronic structures of MX and only one vibrational mode make the assignment of the photoelectron spectrum easier, which also makes it easier to distinguish between the valence-bound state near the detachment threshold and the DBS.[32] For such a simple system, high-level theoretical methods can be employed to calculate the properties of DBSs in comparison with the experimental results. In 1997, Gutsev and co-workers predicted the existence of excited DBSs for some polar diatomic molecules (LiH^-, LiF^-, $LiCl^-$, NaH^-, NaF^-, $NaCl^-$, BeO^-, and MgO^-) using the equation-of-motion coupled-cluster method for electron attachment with single and double substitutions (EOM-EA-CCSD).[33] Among them, we experimentally tried NaCl since it has the largest dipole moment, 9.0 D.[34,35] However, we observed only one DBS, and it was σ-type. Therefore, we turned to molecules with a larger dipole moment.

In this work, we report both σ-type and π-type DBS observation in potassium iodide (KI) anion. The dipole moment of KI was measured to be 10.82(10) D by Story et al.,[36] which well exceeds the critical dipole moment 9.6 D for a π-type DBS derived through the finite dipole model.[28,29] The experiment was carried out on our slow-electron velocity-map imaging (SEVI) apparatus equipped with a cryogenically controlled ion trap.[37−41] The instrument can be switched between the SEVI mode and the scan mode so that we can acquire the photoelectron energy spectra in the SEVI mode and search for resonance peaks by scanning the wavelength of the photodetachment laser in the scan mode. The KI^- anions

Received: May 31, 2021
Accepted: June 17, 2021

© XXXX American Chemical Society

https://doi.org/10.1021/acs.jpclett.1c01726
J. Phys. Chem. Lett. 2021, 12, 5897−5902

were generated via laser ablation of a KI salt disk. The generated anions were guided into the radio frequency ion trap by a hexapole ion guide and then cooled through collisions with the buffer gas (20% H_2 and 80% He) in the ion trap. All spectra in the present work were collected with the ion trap at a nominal temperature of 15 K. After cooling for 45 ms, the anions were pulsed out from the cold trap, and flew into a Wiley–McLaren type time-of-flight (TOF) mass spectrometer.[42] The anions of interest were selected by a mass gate and photodetached in the interaction zone of velocity map imaging (VMI). The detachment laser was either the idler light of an optical parametric oscillator (OPO, 710–2750 nm for the idler light and line width ~5 cm^{-1}) pumped by a Quanta-Ray Lab 190 Nd:YAG or the infrared difference frequency generation (DFG) of a tunable dye laser (400–920 nm) and its residual 1064 nm light. The wavelength of the dye laser was monitored via a wavelength meter (HighFinesse WS6-600, 0.02 cm^{-1} accuracy). The line width of the infrared laser from DFG was about 1 cm^{-1}, limited by the line width of the 1064 nm light.

The electron affinity (EA) value of KI was measured to be 0.728(10) eV by Miller et al.[43] To increase its accuracy, we tuned the photon energy of the photodetachment DFG laser slightly above the EA of KI and determined the EA value to be 5865.2(54) cm^{-1} or 727.19(67) meV. To search for the DBS in KI^-, we scanned the photon energy around the EA of KI and recorded the corresponding photoelectron yield. As shown in Figure 1, we observed nine resonant peaks in the photodetachment spectrum of KI^-. These peaks can be grouped into two nearly equi-spaced series, which are related to two bound states of KI^-. Peaks 1, 2, 4, 6, and 8 belong to one vibrational series with a 178(6) cm^{-1} gap, and peaks 3, 5, 7, and 9 belong to the other vibrational series with an interval of 174(15) cm^{-1}. The vibrational frequency of neutral KI is known to be 186.24(4) cm^{-1} (ref 44) and was measured as 181(14) cm^{-1} from the photoelectron energy spectra in the present work. The similarity between the vibrational frequencies of the two excited states of KI^- and the ground state of KI reveals their similar structure. Thus, the two weakly bound states of KI^- are DBSs. No more resonances were observed when the photon energy was further lowered. Peak 1 and peak 3 should be the vibrational ground states, with the binding energies of 320(8) cm^{-1} or 39.7(10) meV and 40(10) cm^{-1} or 5.0(12) meV, respectively. The resonance peaks below the photodetachment threshold were due to resonant two-photon detachment (R2PD). The KI^- in ground state resonantly absorbed one photon, was excited to a DBS, and was then photodetached by a second photon. When the photon energy was above the EA, the resonant peaks were due to the fast autodetachment after resonantly absorbing one photon.[45]

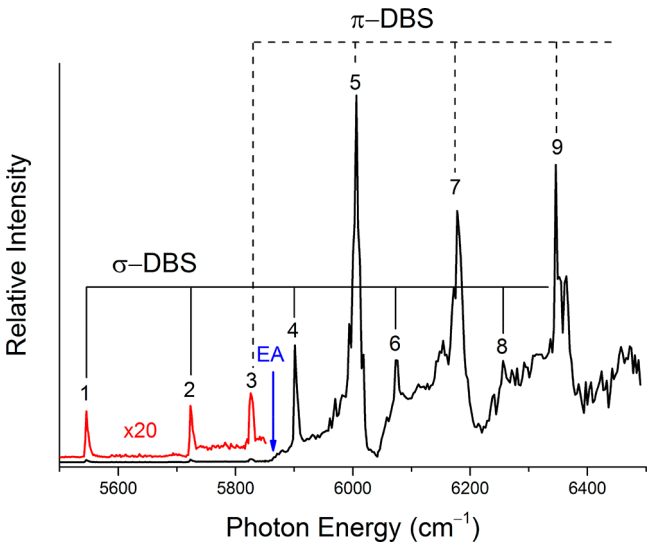

Figure 1. Photodetachment spectrum of KI^- near the photodetachment threshold. The red curve shows the weak peaks multiplied by a factor of 20. The resonant peaks were grouped into two series: σ-type dipole-bound state (DBS) and π-type according to the gaps.

Figure 2 shows the R2PD spectra related to the resonant peaks 1, 2, and 3 using the DFG light. The energy spectra have the typical character of DBS, with a single strong peak at low binding energy. It is interesting to note the different photoelectron angular distributions (PADs) of the DBSs. PADs provide us with information on molecular orbitals to help with the assignment.[46−49] Peak 1 and peak 2 belong to the same vibrational series. In the R2PD spectra of peak 1 and peak 2, the anisotropy parameters (β) for two DBS peaks are 1.5 and 1.4, respectively, which shows the p-wave character of the photoelectrons, suggesting that peaks 1, 2, 4, 6, and 8 are the vibrational series of a σ-type DBS. For the R2PD spectrum of peak 3, β is 0.5, indicating an (s + d)-wave angular distribution, suggesting that peaks 3, 5, 7, and 9 are related to a

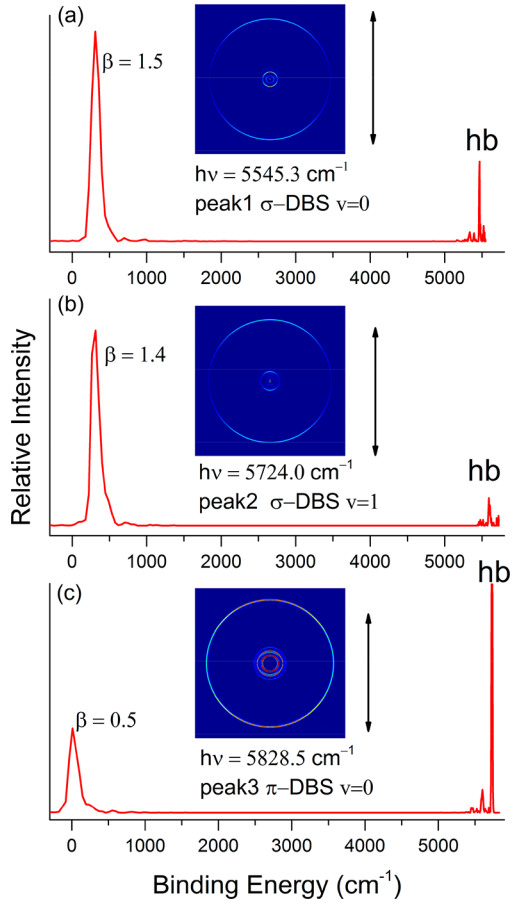

Figure 2. Resonant two-photon detachment spectra and images of KI^- via DBSs. The double arrow indicates the polarization of the photodetachment laser. The label "hb" indicates the vibrational hot band of KI^-.

https://doi.org/10.1021/acs.jpclett.1c01726
J. Phys. Chem. Lett. 2021, 12, 5897−5902

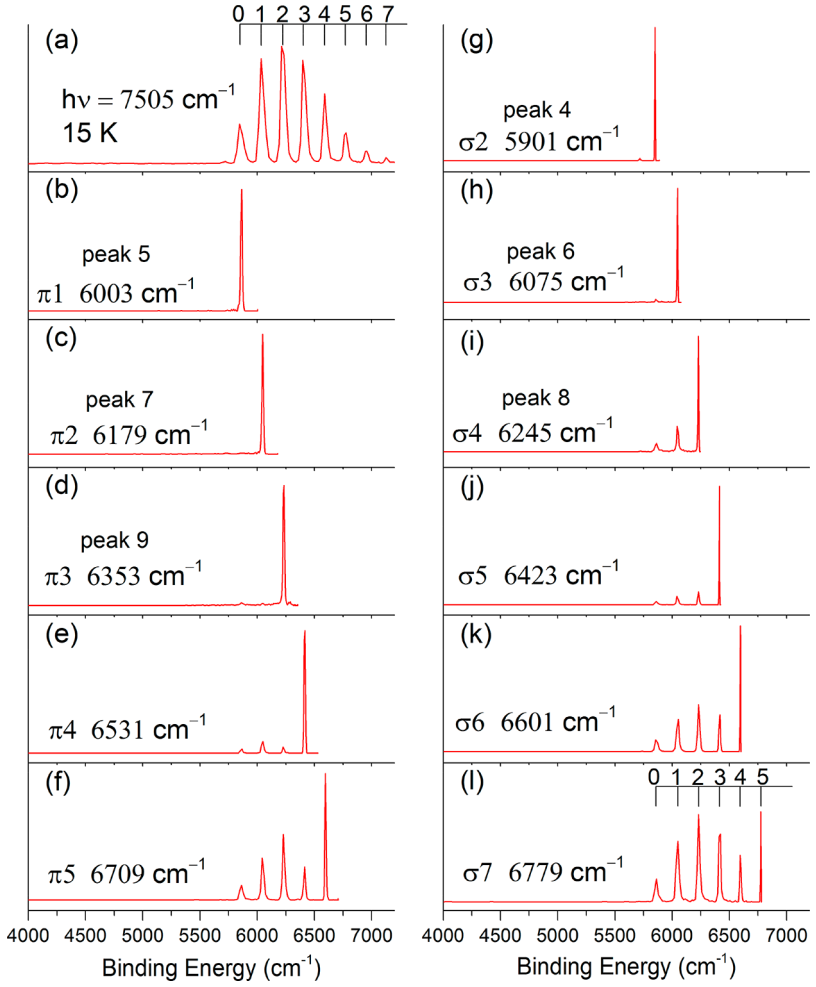

Figure 3. (a) Nonresonant photoelectron energy spectrum of KI^- at $h\nu$ = 7505 cm^{-1}. The panels (b)−(f) are resonant photoelectron energy spectra with different vibrational excited states for the π-type DBS above the photodetachment threshold and (g)−(l) for the σ-type DBS. The spectra (e), (f), and (j)−(l) were acquired at the expected resonant photon energies, which could not be clearly observed in Figure 1 due to the strong background of the direct photodetachment. The vibrational levels are marked at the top in panels (a) and (l).

π-type DBS. This assignment is further supported by the binding energies of DBS peaks in Figure 2. They are the same for Figure 2a,b but different for Figure 2c. The different binding energies are due to the different types of DBSs. The DBS peaks of Figure 2a,b have the same binding energy because the neutral core almost remained intact while the dipole-bound electron was photodetached. The vibrational quantum number v = 0 in Figure 2a, and v = 1 for Figure 2b. There were no changes in the vibrational states, which further confirms that the potential energy curve of KI^- in a DBS is almost parallel with that of KI. The sharp peaks labeled as "hb" at high binding energy in Figure 2 are the "vibrational hot bands" of KI^-. The "hb" have two contributions: one from the thermal population at the ion temperature ∼30 K and the other from the R2PD processes; some of the excited vibrational states are populated via the relaxation from the DBS after absorbing the first photon. The vibrational frequency of KI^- was determined to be 134(17) cm^{-1} according to the hot bands.

Figure 3 shows the resonant photoelectron energy spectra of KI^- in comparison with the nonresonant photoelectron energy spectrum with a photon energy $h\nu$ = 7505 cm^{-1}. The photon energy was tuned to the resonances via the π-type DBS with the vibrational quantum number v = 1−5 in Figure 3b−f and the σ-type DBS with v = 2−7 in Figure 3g−l. The anion in its ground state was excited to the vibrational excited state of a DBS by resonantly absorbing one photon and then quickly autodetached due to the vibronic coupling. It can be seen that the peaks with the lowest kinetic energy were resonantly enhanced in every spectrum of Figure 3b−l, which reveals the propensity rule $\Delta v = -1$ for the vibrational-induced autodetachment from π-type DBS[50−54] and $\Delta v = -2$ for σ-type. $\Delta v = -2$ violated the general rule $\Delta v = -1$ for the autodetachment of a DBS.[32,55,56] This is due to the higher binding energy of the σ-type DBS in KI^-. One quantum of the vibrational energy is not high enough to detach σ-type DBS. Since the potential curve of DBS is almost parallel with the neutral, the Franck−Condon factor for $\Delta v = -2$ is significantly less than that for $\Delta v = -1$. This can explain why the resonant peaks for σ-type DBS are much weaker than that for π-type in Figure 1.

To further understand the DBSs of KI^-, we performed calculations using EOM-EA-CCSD[57−59] via the Q-Chem program.[60] The basis sets were aug-cc-pVTZ-PP[61,62] + 6s6p3d for K and aug-cc-pVTZ-PP[63] + 6s6p3d for I. The extra diffuse functions were added in an even-tempered manner. The bond length of KI^- in the σ-type DBS was optimized as 3.032 Å. Indeed, our calculations showed the

https://doi.org/10.1021/acs.jpclett.1c01726
J. Phys. Chem. Lett. 2021, 12, 5897−5902

existence of two DBSs with binding energies of 39.1 meV (σ-type DBS) and 4.7 meV (π-type DBS), which are in excellent agreement with the experimental results 39.7(10) meV and 5.0(12) meV. This further confirms our assignment. The molecular orbitals and energy levels related to DBSs are illustrated in Figure 4.

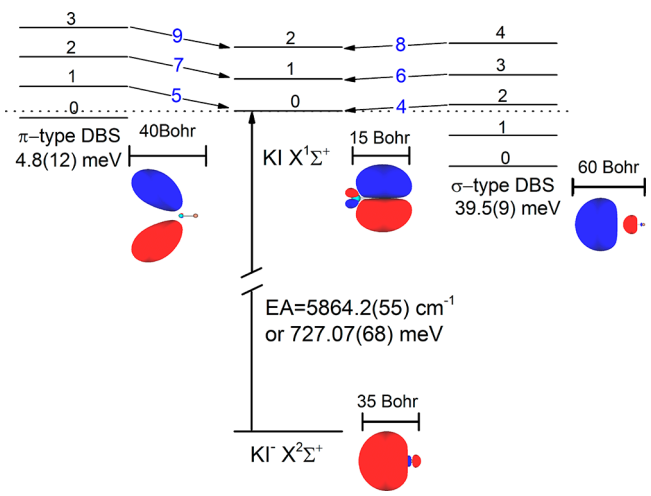

Figure 4. Molecular orbitals (MO) and vibrational energy levels of KI and KI^- in DBS. All MOs were plotted with the same contour value of 0.003 but in different scales indicated by the scale bars for a better view. The highest occupied molecular orbital (HOMO) of KI in the ground state ($X^1\Sigma^+$) was also plotted for comparison. The potassium atom is on the left.

The diffuse DBS is an analogue to the Rydberg state.[64] In contrast to the positively charged core of the Rydberg state in neutral atoms and positive ions, the core of a DBS is a neutral dipole. The existence of the σ-type and π-type DBS in a diatomic anion could provide a new platform to investigate the dipolar interaction once the diatomic anion can be cooled down to an ultracold temperature.[65] Laser cooling of some polar molecules has been realized recently, such as YO[66] and SrF.[67] With Rydberg electron transfer to these laser cooled molecules,[68] it may be possible to create ultracold dipolar negative ions.

In conclusion, we directly observed both σ-type and π-type dipole-bound states in the KI^- anion, and the binding energies were determined to be 320(8) cm^{-1} or 39.7(10) meV and 40(10) cm^{-1} or 5.0(12) meV, respectively. The assignment of the observation was supported by the photoelectron angular distributions of the two-photon resonant photodetachment and the energy spectra. Furthermore, we have confirmed the existence of one σ-type and one π-type excited DBS through high-level calculations using the EOM-EA-CCSD method. The measured and calculated binding energies are in excellent agreement, demonstrating the power of the combination of the cryo-SEVI measurement and the high-level calculation for investigating the very diffuse dipole-bound states.

AUTHOR INFORMATION

Corresponding Author

Chuangang Ning − *Department of Physics, State Key Laboratory of Low Dimensional Quantum Physics, Tsinghua University, Beijing 10084, China; Collaborative Innovation Center of Quantum Matter, Beijing 100871, China;* orcid.org/0000-0002-3158-1253; Email: ningcg@tsinghua.edu.cn

Authors

Yuzhu Lu − *Department of Physics, State Key Laboratory of Low Dimensional Quantum Physics, Tsinghua University, Beijing 10084, China*

Rulin Tang − *Department of Physics, State Key Laboratory of Low Dimensional Quantum Physics, Tsinghua University, Beijing 10084, China*

Complete contact information is available at: https://pubs.acs.org/10.1021/acs.jpclett.1c01726

Notes

The authors declare no competing financial interest.

ACKNOWLEDGMENTS

This work is supported by the National Natural Science Foundation of China (NSFC) (Grant No. 11974199) and the National key R&D program of China (2018YFA0306504).

REFERENCES

(1) Desfrançois, C.; Abdoul-Carime, H.; Schermann, J.-P. Ground-state dipole-bound anions. *Int. J. Mod. Phys. B* **1996**, *10* (12), 1339−1395.

(2) Compton, R.; Hammer, N. Advances in gas-phase ion chemistry. *Adv. Gas Phase Ion Chem.* **2001**, *4*, 257−291.

(3) Jordan, K. D.; Wang, F. Theory of dipole-bound anions. *Annu. Rev. Phys. Chem.* **2003**, *54* (1), 367−396.

(4) Simons, J. Molecular anions. *J. Phys. Chem. A* **2008**, *112* (29), 6401−6511.

(5) Qian, C.-H.; Zhu, G.-Z.; Wang, L.-S. Probing the Critical Dipole Moment To Support Excited Dipole-Bound States in Valence-Bound Anions. *J. Phys. Chem. Lett.* **2019**, *10* (21), 6472−6477.

(6) Compton, R.; Carman, H., Jr; Desfrançois, C.; Abdoul-Carime, H.; Schermann, J.; Hendricks, J.; Lyapustina, S.; Bowen, K. On the binding of electrons to nitromethane: Dipole and valence bound anions. *J. Chem. Phys.* **1996**, *105* (9), 3472−3478.

(7) Sommerfeld, T. Coupling between dipole-bound and valence states: the nitromethane anion. *Phys. Chem. Chem. Phys.* **2002**, *4* (12), 2511−2516.

(8) Hendricks, J.; Lyapustina, S.; De Clercq, H.; Bowen, K. The dipole bound-to-covalent anion transformation in uracil. *J. Chem. Phys.* **1998**, *108* (1), 8−11.

(9) Sommerfeld, T. Doorway mechanism for dissociative electron attachment to fructose. *J. Chem. Phys.* **2007**, *126* (12), 124301.

(10) Eustis, S. N.; Radisic, D.; Bowen, K. H.; Bachorz, R. A.; Haranczyk, M.; Schenter, G. K.; Gutowski, M. Electron-Driven Acid-Base Chemistry: Proton Transfer from Hydrogen Chloride to Ammonia. *Science* **2008**, *319* (5865), 936.

(11) Hendricks, J. H.; Lyapustina, S. A.; de Clercq, H. L.; Snodgrass, J. T.; Bowen, K. H. Dipole bound, nucleic acid base anions studied via negative ion photoelectron spectroscopy. *J. Chem. Phys.* **1996**, *104* (19), 7788−7791.

(12) Smith, D. M. A.; Smets, J.; Adamowicz, L. Anions of the Hydrogen-Bonded Uracil Dimer. Ab Initio Theoretical Study. *J. Phys. Chem. A* **1999**, *103* (29), 5784−5790.

(13) King, S. B.; Stephansen, A. B.; Yokoi, Y.; Yandell, M. A.; Kunin, A.; Takayanagi, T.; Neumark, D. M. Electron accommodation dynamics in the DNA base thymine. *J. Chem. Phys.* **2015**, *143* (2), 024312.

(14) Kunin, A.; Neumark, D. M. Time-resolved radiation chemistry: femtosecond photoelectron spectroscopy of electron attachment and photodissociation dynamics in iodide−nucleobase clusters. *Phys. Chem. Chem. Phys.* **2019**, *21* (14), 7239−7255.

(15) Desfrançois, C.; Abdoul-Carime, H.; Schermann, J. P. Electron attachment to isolated nucleic acid bases. *J. Chem. Phys.* **1996**, *104* (19), 7792−7794.
(16) Guthe, F.; Tulej, M.; Pachkov, M. V.; Maier, J. P. Photodetachment Spectrum of l-$C_3H_2^-$: The Role of Dipole Bound States for Electron Attachment in Interstellar Clouds. *Astrophys. J.* **2001**, *555* (1), 466−471.
(17) Fortenberry, R. C. Interstellar Anions: The Role of Quantum Chemistry. *J. Phys. Chem. A* **2015**, *119* (39), 9941−9953.
(18) Fermi, E.; Teller, E. The Capture of Negative Mesotrons in Matter. *Phys. Rev.* **1947**, *72* (5), 399−408.
(19) Turner, J. Minimum dipole moment required to bind an electron-molecular theorists rediscover phenomenon mentioned in Fermi-Teller paper twenty years earlier. *Am. J. Phys.* **1977**, *45* (8), 758−766.
(20) Crawford, O. H. Negative ions of polar molecules. *Mol. Phys.* **1971**, *20* (4), 585−591.
(21) Desfrançois, C.; Abdoul-Carime, H.; Khelifa, N.; Schermann, J. From 1/r to $1/r^2$ Potentials: Electron Exchange between Rydberg Atoms and Polar Molecules. *Phys. Rev. Lett.* **1994**, *73* (18), 2436.
(22) Hammer, N. I.; Diri, K.; Jordan, K. D.; Desfrançois, C.; Compton, R. N. Dipole-bound anions of carbonyl, nitrile, and sulfoxide containing molecules. *J. Chem. Phys.* **2003**, *119* (7), 3650−3660.
(23) Hammer, N. I.; Hinde, R. J.; Compton, R. N.; Diri, K.; Jordan, K. D.; Radisic, D.; Stokes, S. T.; Bowen, K. H. Dipole-bound anions of highly polar molecules: Ethylene carbonate and vinylene carbonate. *J. Chem. Phys.* **2004**, *120* (2), 685−690.
(24) Garrett, W. R. Excited states of polar negative ions. *J. Chem. Phys.* **1982**, *77* (7), 3666−3673.
(25) Clary, D. C. Photodetachment of electrons from dipolar anions. *J. Phys. Chem.* **1988**, *92* (11), 3173−3181.
(26) Clary, D. C.; Henshaw, J. P. Reaction rates of electrons with dipolar molecules. *Int. J. Mass Spectrom. Ion Processes* **1987**, *80*, 31−49.
(27) Huang, D.-L.; Zhu, G.-Z.; Liu, Y.; Wang, L.-S. Photodetachment spectroscopy and resonant photoelectron imaging of cryogenically-cooled deprotonated 2-hydroxypyrimidine anions. *J. Mol. Spectrosc.* **2017**, *332*, 86−93.
(28) Wallis, R. F.; Herman, R.; Milnes, H. W. Energy levels of an electron in the field of a finite dipole. *J. Mol. Spectrosc.* **1960**, *4* (1−6), 51−74.
(29) Crawford, O. H. Bound states of a charged particle in a dipole field. *Proc. Phys. Soc., London* **1967**, *91*, 279.
(30) Yuan, D.-F.; Liu, Y.; Qian, C.-H.; Zhang, Y.-R.; Rubenstein, B. M.; Wang, L.-S. Observation of a π-type dipole-bound state in molecular anions. *Phys. Rev. Lett.* **2020**, *125* (7), 073003.
(31) Yuan, D.-F.; Zhang, Y.-R.; Qian, C.-H.; Liu, Y.; Wang, L.-S. Probing the Dipole-Bound State in the 9-Phenanthrolate Anion by Photodetachment Spectroscopy, Resonant Two-Photon Photoelectron Imaging, and Resonant Photoelectron Spectroscopy. *J. Phys. Chem. A* **2021**, *125* (14), 2967−2976.
(32) Lu, Y.; Tang, R.; Fu, X.; Liu, H.; Ning, C. Dipole-bound and valence excited states of AuF anions via resonant photoelectron spectroscopy. *J. Chem. Phys.* **2021**, *154* (7), 074303.
(33) Gutsev, G. L.; Nooijen, M.; Bartlett, R. J. Valence and excited dipole-bound states of polar diatomic anions: LiH^-, LiF^-, $LiCl^-$, NaH^-, NaF^-, $NaCl^-$, BeO^-, and MgO^-. *Chem. Phys. Lett.* **1997**, *276* (1), 13−19.
(34) Hebert, A.; Lovas, F.; Melendres, C.; Hollowell, C.; Story, T., Jr; Street, K., Jr Dipole moments of some alkali halide molecules by the molecular beam electric resonance method. *J. Chem. Phys.* **1968**, *48* (6), 2824−2825.
(35) De Leeuw, F.; Van Wachem, R.; Dymanus, A. Radio-Frequency Spectra of NaCl by the Molecular-Beam Electric Resonance Method. *J. Chem. Phys.* **1970**, *53* (3), 981−984.
(36) Story, T. L., Jr.; Hebert, A. J. Dipole moments of KI, RbBr, RbI, CsBr, and CsI by the electric deflection method. *J. Chem. Phys.* **1976**, *64* (2), 855−858.
(37) Chen, X.-L.; Ning, C.-G. Accurate electron affinity of Co and fine-structure splittings of Co^- via slow-electron velocity-map imaging. *Phys. Rev. A: At., Mol., Opt. Phys.* **2016**, *93* (5), 052508.
(38) Tang, R.-L.; Fu, X.-X.; Ning, C.-G. Accurate electron affinity of Ti and fine structures of its anions. *J. Chem. Phys.* **2018**, *149* (13), 134304.
(39) Hock, C.; Kim, J. B.; Weichman, M. L.; Yacovitch, T. I.; Neumark, D. M. Slow photoelectron velocity-map imaging spectroscopy of cold negative ions. *J. Chem. Phys.* **2012**, *137* (24), 244201.
(40) León, I.; Yang, Z.; Liu, H.-T.; Wang, L.-S. The design and construction of a high-resolution velocity-map imaging apparatus for photoelectron spectroscopy studies of size-selected clusters. *Rev. Sci. Instrum.* **2014**, *85* (8), 083106.
(41) Tang, R.; Si, R.; Fei, Z.; Fu, X.; Lu, Y.; Brage, T.; Liu, H.; Chen, C.; Ning, C. Observation of electric-dipole transitions in the laser-cooling candidate Th^- and its application for cooling antiprotons. *Phys. Rev. A: At., Mol., Opt. Phys.* **2021**, *103* (4), 042817.
(42) Wiley, W. C.; McLaren, I. H. Time-of-Flight Mass Spectrometer with Improved Resolution. *Rev. Sci. Instrum.* **1955**, *26* (12), 1150−1157.
(43) Miller, T. M.; Leopold, D. G.; Murray, K. K.; Lineberger, W. C. Electron affinities of the alkali halides and the structure of their negative ions. *J. Chem. Phys.* **1986**, *85* (5), 2368−2375.
(44) Rusk, J. R.; Gordy, W. Millimeter Wave Molecular Beam Spectroscopy: Alkali Bromides and Iodides. *Phys. Rev.* **1962**, *127* (3), 817−830.
(45) Kang, D. H.; An, S.; Kim, S. K. Real-Time Autodetachment Dynamics of Vibrational Feshbach Resonances in a Dipole-Bound State. *Phys. Rev. Lett.* **2020**, *125* (9), 093001.
(46) Cooper, J.; Zare, R. N. Angular Distribution of Photoelectrons. *J. Chem. Phys.* **1968**, *48* (2), 942−943.
(47) Cooper, J.; Zare, R. Angular Distributions in Atomic Anion Photodetachment (Erratum). *J. Chem. Phys.* **1968**, *49*, 4252.
(48) Sanov, A. Laboratory-frame photoelectron angular distributions in anion photodetachment: insight into electronic structure and intermolecular interactions. *Annu. Rev. Phys. Chem.* **2014**, *65*, 341−363.
(49) Simons, J. Ejecting Electrons from Molecular Anions via Shine, Shake/Rattle, and Roll. *J. Phys. Chem. A* **2020**, *124* (42), 8778−8797.
(50) Simons, J. Propensity rules for vibration-induced electron detachment of anions. *J. Am. Chem. Soc.* **1981**, *103* (14), 3971−3976.
(51) Acharya, P.; Kendall, R. A.; Simons, J. Vibration-induced electron detachment in molecular anions. *J. Am. Chem. Soc.* **1984**, *106* (12), 3402−3407.
(52) Wetzel, D. M.; Brauman, J. I. Rotational structure in an excited vibronic band of the dipole-supported state of cyanomethyl anion, CH2CN$^-$. *J. Chem. Phys.* **1989**, *90* (1), 68−73.
(53) Liu, H. T.; Ning, C. G.; Huang, D. L.; Dau, P. D.; Wang, L. S. Observation of Mode-Specific Vibrational Autodetachment from Dipole-Bound States of Cold Anions. *Angew. Chem., Int. Ed.* **2013**, *52* (34), 8976−8979.
(54) Liu, H. T.; Ning, C. G.; Huang, D. L.; Wang, L. S. Vibrational Spectroscopy of the Dehydrogenated Uracil Radical by Autodetachment of Dipole-Bound Excited States of Cold Anions. *Angew. Chem., Int. Ed.* **2014**, *53* (9), 2464−2468.
(55) Zhu, G.-Z.; Qian, C.-H.; Wang, L.-S. Dipole-bound excited states and resonant photoelectron imaging of phenoxide and thiophenoxide anions. *J. Chem. Phys.* **2018**, *149* (16), 164301.
(56) Zhu, G.-Z.; Wang, L.-S. High-resolution photoelectron imaging and resonant photoelectron spectroscopy via noncovalently bound excited states of cryogenically cooled anions. *Chem. Sci.* **2019**, *10* (41), 9409−9423.
(57) Krylov, A. I. Equation-of-motion coupled-cluster methods for open-shell and electronically excited species: The hitchhiker's guide to Fock space. *Annu. Rev. Phys. Chem.* **2008**, *59*, 433.
(58) Sneskov, K.; Christiansen, O. Excited state coupled cluster methods. *Wiley Interdiscip. Rev. Comput. Mol. Sci.* **2012**, *2* (4), 566−584.

https://doi.org/10.1021/acs.jpclett.1c01726
J. Phys. Chem. Lett. 2021, 12, 5897−5902

(59) Nooijen, M.; Bartlett, R. J. Equation of motion coupled cluster method for electron attachment. *J. Chem. Phys.* **1995**, *102* (9), 3629−3647.
(60) Shao, Y.; Gan, Z.; Epifanovsky, E.; Gilbert, A. T.; Wormit, M.; Kussmann, J.; Lange, A. W.; Behn, A.; Deng, J.; Feng, X.; et al. Advances in molecular quantum chemistry contained in the Q-Chem 4 program package. *Mol. Phys.* **2015**, *113* (2), 184−215.
(61) Hill, J. G.; Peterson, K. A. Gaussian basis sets for use in correlated molecular calculations. XI. Pseudopotential-based and all-electron relativistic basis sets for alkali metal (K−Fr) and alkaline earth (Ca−Ra) elements. *J. Chem. Phys.* **2017**, *147* (24), 244106.
(62) Lim, I. S.; Schwerdtfeger, P.; Metz, B.; Stoll, H. All-electron and relativistic pseudopotential studies for the group 1 element polarizabilities from K to element 119. *J. Chem. Phys.* **2005**, *122* (10), 104103.
(63) Peterson, K. A.; Shepler, B. C.; Figgen, D.; Stoll, H. On the spectroscopic and thermochemical properties of ClO, BrO, IO, and their anions. *J. Phys. Chem. A* **2006**, *110* (51), 13877−13883.
(64) Saffman, M.; Walker, T. G.; Mølmer, K. Quantum information with Rydberg atoms. *Rev. Mod. Phys.* **2010**, *82* (3), 2313.
(65) DeMille, D. Quantum computation with trapped polar molecules. *Phys. Rev. Lett.* **2002**, *88* (6), 067901.
(66) Ding, S.; Wu, Y.; Finneran, I. A.; Burau, J. J.; Ye, J. Sub-Doppler Cooling and Compressed Trapping of YO Molecules at μ K Temperatures. *Phys. Rev. X* **2020**, *10* (2), 021049.
(67) Shuman, E. S.; Barry, J. F.; DeMille, D. Laser cooling of a diatomic molecule. *Nature* **2010**, *467* (7317), 820−823.
(68) Ciborowski, S. M.; Liu, G.; Graham, J. D.; Buytendyk, A. M.; Bowen, K. H. Dipole-bound anions: formed by Rydberg electron transfer (RET) and studied by velocity map imaging−anion photoelectron spectroscopy (VMI−aPES). *Eur. Phys. J. D* **2018**, *72* (8), 1−5.

https://doi.org/10.1021/acs.jpclett.1c01726
J. Phys. Chem. Lett. 2021, 12, 5897−5902